Quantitative Laser Raman Analysis of Mixed Gases from the Seafloor

Kennedy McCone, Stanford University

Mentors: Peter Brewer, Edward Peltzer, Peter Walz

Summer 2015

Keywords: Eel River Canyon, methane, hydrocarbons, laser Raman spectroscopy, gas

ABSTRACT

The use of laser Raman spectroscopy (LRS) to explore the physical and geochemistry of the deep sea has escalated during the past fifteen years due to developments in the stability of the LRS hardware in the ocean. This project explored the practicality and utility of making laboratory laser Raman measurements of deep sea gases. Samples consisted of mixed gases originating from Eel River Canyon vents at the North and South Slump sites. The construction of a pressure boosting system enabled detection of trace gases, including multiple-carbon alkanes, carbon dioxide, and nitrogen. A series of calibration curves that plotted peak height ratios against molar ratios from standard gases allowed for quantitative measurements of the molar composition of the samples, with less than 1% uncertainty in the ethane to methane ratio. Complete analysis revealed that samples contained between 89 and 98% methane, with slight variations in composition that displayed some temporal and spatial patterns. Comparisons of the laboratory measurements of the free gases to in-situ spectra of free gas, gas dissolved in oil, and hydrates from Eel River Canyon illuminate avenues for further research.

INTRODUCTION

Laser Raman spectroscopy (LRS) has become a powerful tool for studying the chemistry of ocean materials in-situ in the last fifteen years (Zhang 2012). In LRS, the laser light interacts with vibrational modes of molecules with polarizable bonds. These interactions shift the frequencies of some of the incident photons in a phenomenon called "Raman scattering"; the shifts are characteristic of the molecules and their immediate environment and can be used to identify sample composition in resulting spectra.

The Brewer group at the Monterey Bay Aquarium Research Institute (MBARI) has pioneered the use of LRS in the deep sea by developing two models of Deep Ocean Raman In Situ Spectrometers (DORISS) (Zhang 2012). In accordance with a larger goal of MBARI to advance better instruments and methods for research in the ocean environment, DORISS1 and DORISS2 have enabled the geochemical study of materials under natural pressure and temperature conditions. Natural gas hydrates, which lose stability before reaching the higher temperature and low pressure conditions of the sea surface, are a primary target of in-situ LRS studies. LRS has proved a useful technique for probing transparent of semi-transparent targets that do not require extremely precise focusing of the laser, such as pore waters, and gases emanating from subsurface vents (Walz 2014). LRS provides several advantages over other analytical techniques, including the ability to take measurements at different points on a sample and its non-destructive and non-invasive nature (Brewer 2004). The near-instantaneous nature of acquiring Raman spectrum is ideal on remotely operated vehicle (ROV) missions because it allows a science team to make decisions during a dive that can help the team make the most of an expedition (Zhang 2012).

The objective of this research project was to develop a laboratory method for performing laser Raman analysis on gases collected from the seafloor of Eel River Canyon, off the coast of Northern California. This provides validation and

correction of in situ measurements through the greater control of critical experimental variables.

In addition to method development, this project also provided the opportunity to characterize the gases and decomposed hydrates from Eel River Canyon. This is a region of great interest to the scientific and commercial worlds alike due to the presence of natural gas vents, oil seeps, and hydrate outcroppings (Walz 2014). Unique geological and acoustic features, chemosynthetic life forms, stable methane hydrates, and potential variations in flux and composition of seep effluent present just a few of the points of investigations at seep sites like Eel River Canyon (Hovland 2012). Studying the rise of oil and venting gas from these natural seeps illuminates the effects of the potential release of large amounts of methane from hydrates as the ocean temperature rises (MBARI 2013 Annual Report, Rehder 2009). Past scientific studies at gas seeps have involved the dissolution rate of methane from a bubble and delivery of methane from the seafloor to the atmosphere (Rehder 2009). The existence of many methane seeps within the hydrate stability zone has also enabled detailed observations of the physical structure of hydrates and hydrate skins on gas bubbles (Rehder 2012). With respect to commercial interest, a complex gas mixture can indicate a thermogenic source and the presence of petroleum.

In 2009, scientists from the University of New Hampshire and the National Oceanic and Atmospheric Administration discovered the gas vents offshore of Eel River as an acoustic anomaly on their SONAR display (Gardner 2009). A team from MBARI traveled to the offshore Eel River Canyon in 2011 to perform high resolution multi-beam bathymetry mapping with an autonomous underwater vehicle (Walz 2014, Gwiazda 2011). Near 40.5355 °N 124.7847 °W and 1813 below the surface, they found “Eel Slump South,” a sixty meter high, two kilometer long mound (Walz 2014). Atop the South Slump are a large depression and various pockmarks that led the team to suspect hydrate deposits and gas vents lay nearby (Gwiazda 2011). The MBARI team also discovered “Eel Slump North” at 40.6645 °N 124.7603 °W and 1623 meters depth (Walz 2014). The North Slump lies at the foot of a scarp with walls containing exposed hydrate

and a hummocky geology that suggested the presence of gas vents (Gwiazda 2011).

ROV dives during the original expedition and subsequent MBARI trips confirmed the suspected presence of methane hydrates, oil-containing sediments, and gas vents using DORISS2 and push core samples (Walz 2014). The Brewer group performed a special experiment in which they acquired multiple in-situ spectra of gas evolving from the oil as the ROV ascended to shallower depths. Laser Raman spectra revealed the North Slump hydrate to be pure sI methane hydrate, while specimens from the South Slump were sII and appeared to contain trace amounts of ethane and hydrogen sulfide (Walz 2014). Stronger fluorescence background in the spectra of the South Slump hydrate might signify complex hydrocarbon gases and oils nearby (Walz 2014). The possibility of complexity in the gases elicited interest in collecting samples in 2014 for a more in-depth, laboratory Raman study. With the awareness that LRS cannot detect trace components as well as other analytical techniques such as gas chromatography, the Brewer group desired a method to increase the pressure of the samples to obtain greater signals (Walz 2014).

MATERIALS AND METHODS

1. SAMPLE COLLETION

MBARI scientists acquired samples from the North and South Slumps at Eel River Canyon on the research vessel *Western Flyer* in 2014 and 2013. The ROV *Doc Ricketts* dove to depths of 1623 m and 1813 m with the heated funnel, a device developed by the Brewer laboratory, to collect gases and decomposed hydrates at these sites (Figure 1). The ROV manipulator arm positioned the funnel over a gas vent while the ROV sat on the seafloor. As gas bubbled into the funnel, a hydrate skin formed around the bubbles. The heating element inside the device decomposed these hydrates once at least 150 mL of gas had filled the funnel in order to allow clean flow of gas into evacuated sample cylinders. A piston that

turned a four-way valve controlled opening and closing of pressure cylinders at depth.

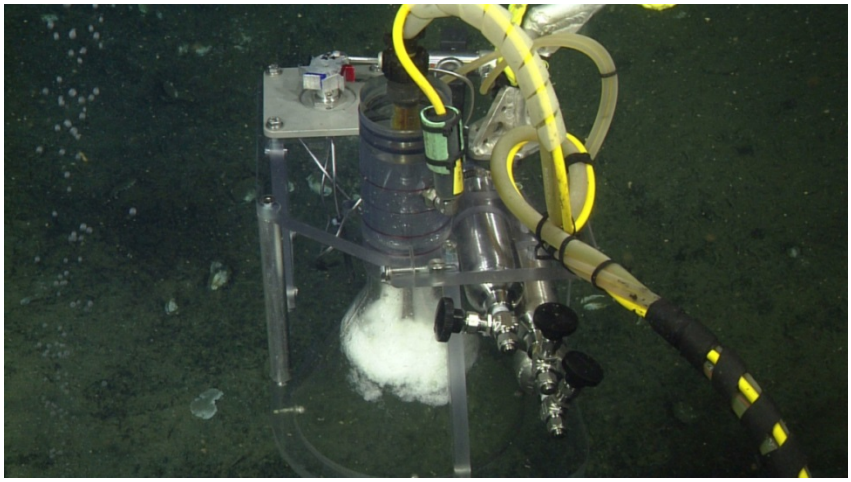

Figure 1 – The heated funnel collects gas bubbling from vents. A heating element in the funnel decomposes the hydrate skins that form around the bubbles.

2. ACQUIRING LABORATORY SPECTRA

A system of valves and stainless steel tubing was used to pressurize standard and sample gases to detect trace components and decrease baseline noise in spectra (Figure 2). Swagelok manufactured all fittings and valves. Needle valves were chosen to control gas flow. Eighth-inch diameter stainless steel tubing connected all components of the system, which included a port to connect the sample cylinder, a pressure booster fabricated in-house at MBARI, a water bath to control temperature, digital pressure and temperature gauges, a vacuum pump and digital vacuum gauge, and a pressure cell. Sam O. Colgate, Inc. fabricated the high-pressure low-temperature Raman cell with stainless steel hardened to the H900 condition, 1/8” diameter stainless steel fill tubes, and single crystal sapphire window.

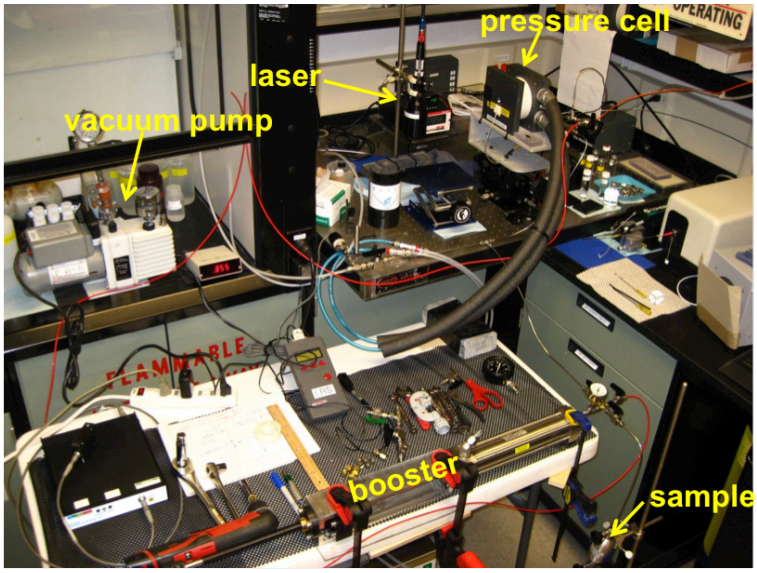

Figure 2 – A network of stainless steel tubing connects the sample cylinder to the pressure booster. The pressure cell allows Raman probing of the sample through a sapphire window. Digital gauges monitored the temperature, pressure, and vacuum.

After evacuating the entire system to 0.14 Torr, a spectrum of the blank cell was acquired to confirm the absence of air and previous sample gas in the pressure cell. The sample cylinder was then opened to the pressure booster. Gradually compressing the gas volume with the booster ram increased the pressure of the gas. Once the gas had reached a sufficiently high pressure, as determined by a mechanical gauge, a needle valve was opened releasing the gas to the pressure cell and the digital pressure gauge. Laser Raman spectra were acquired through the sapphire window of the pressure cell at 400.0, 600.0, 800.0, 1000.0, and 1200.0 psig at 20.0 °C. Each pressure step was achieved by further driving the ram into the pressure booster. Acquisitions consisted of 32 accumulations of 2 second exposures.

Laser Raman spectra were acquired using MBARI's DORISS1 system removed from its deep sea pressure housing. DORISS1 is based on the Holoprobe™ Raman analyzer from Kaiser Optical Systems, Inc. (KOSI) and includes a Holospec f/1.8i spectrometer with a duplex holographic grating and a liquid-cooled, 2048 x 512 charge coupled device (CCD) camera from Andor Technology. The spectral range of the instrument is 100-4400 cm^{-1} and the resolution is 0.3 cm^{-1}. A Nd:YAG 532 nm laser and the spectrometer are

connected to a holographically filtered probe head accommodated in a stand-off sampling optic.

The spectrometer was calibrated for wavelength and intensity with neon and tungsten lamps, respectively, each day before sample analysis. Measuring the laser power at the focal point daily to ensure that it had reached a minimum of 30.0 mW helped maintain consistency in sample analysis. HoloGRAMS software developed by KOSI was used for calibration and spectral acquisition. GRAMS/AI software from Thermo Electron Corp. was used to view spectra and export them to .asc format for further analysis with MATLAB.

3. PROCESSING SPECTRA

A MATLAB script was developed to flatten the baselines and to deconvolute the methane υ_1 stretch that dominated the spectra and overlapped with CH stretches from other alkanes in the gas mixtures (Figure 3). Spectra acquired at 1200.0 psig had the greatest signal to noise ratios and were used for all analyses. To smooth the baselines, the script subtracted the minimum intensity of an entire spectrum from the intensity at each wavenumber value. To deconvolute the methane peak, the routine subtracted a reference spectrum of >99% methane (with ~0.5% nitrogen and traces of C_2-C_4 alkanes) at 1200.0 psi from the original sample spectrum. The methane spectrum was first scaled to match the peak heights of the υ_1 stretch. Then, the methane trace was manually shifted in wavenumbers and scaled in intensity to minimize the methane υ_1 stretch in the difference spectrum. The wavenumber shift was occasionally necessary due to slight variations in peak placement depending on the nature of the gas mixture. The significant presence of gases other than methane in the samples necessitated the scaling factor to decrease

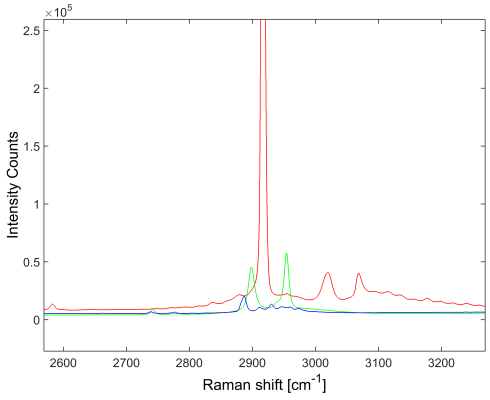

Figure 3 – The methane (red) trace overlaps with other alkanes such as ethane (green) and propane (blue) in the CH stretching region.

the υ_1 methane peak in the 99% methane standard to the appropriate height. The wavenumber offset ranged from 0 to 0.6 cm^{-1}; scaling factors ranged from 0.950 to 1.

After baseline smoothing and methane deconvolution, the MATLAB script calculated separate baselines under each peak of interest by averaging the wavenumbers and intensities in small windows on either side of a peak and calculating a line that intersected both points. The routine then calculated peak height as the distance from the baseline to the corresponding peak maximum intensity. The output of the script was a plot displaying the sample, scaled methane, and difference spectra, the calculated baselines, and a list of resulting peak heights (Figure 4). All peak heights, with the exception of methane and oxygen, were calculated from the original sample spectrum. The methane υ_1 peak height was determined from the appropriately scaled methane trace. The oxygen peak, due to its overlap with the methane υ_1 stretching mode, was calculated from the difference spectrum, which was free of methane peaks. Spectra of standard gases and referencing the National Standard Reference Data System (NSRDS-NBS 39) allowed for identification of peaks (Table 1).

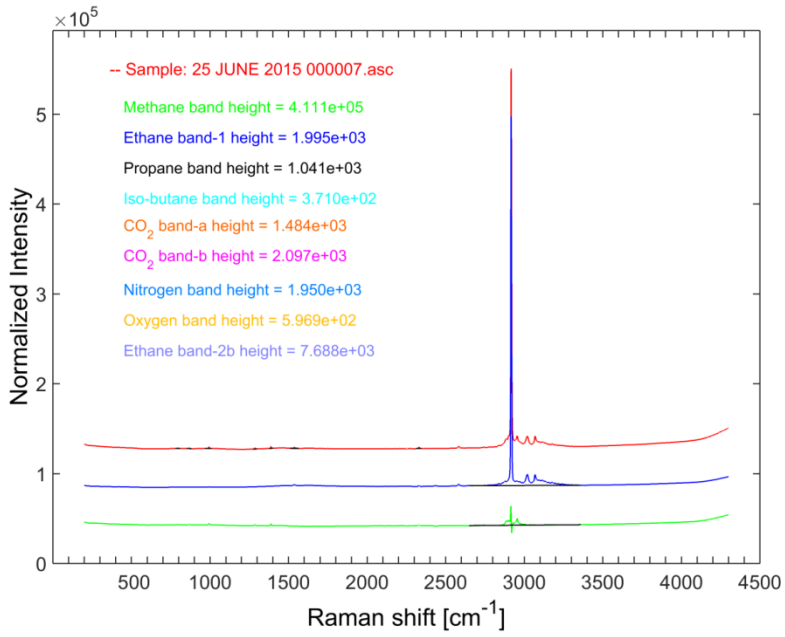

Figure 4 – The output of the MATLAB script plotted the sample, methane, and difference spectra along with the calculated baselines for each peak of interest. It also listed the relevant peak heights.

Table 1 – The Raman shifts of each peak of interest in the acquired spectra. Peak identification resulted from referencing standards as well as NSRDS-NBS 39.

Molecule	**Vibrational mode**	**Raman Shift (cm^{-1})**
Methane	υ_1 symmetric stretch	2916
Ethane	υ_3 CC stretch	993
Propane	υ_8 CC stretch	869
Iso-butane	υ_{10} CC stretch	798
Carbon dioxide	$2\upsilon_2$ bend υ_1 symmetric stretch	1285 1388
Nitrogen	υ_0	2330
Oxygen	υ_0	1556

RESULTS

1. OBTAINING MOLAR RATIOS FROM PEAK HEIGHTS

Peak height served as the best metric for quantitatively analyzing laser Raman spectra of the mixed gas samples due to the linear relationship between peak height and pressure for all detected gas components. Plotting peak height against absolute pressure for a series of standards and calculating linear regressions produced R^2 values of over 0.998 (Figure 5). For carbon dioxide, plotting the sum of the two peak heights against pressure gave a linear response with R^2 = 0.990, as did the nitrogen peak height. The calculated oxygen peak height was not as linear due to the partial overlap with the methane υ_2 stretching mode. All oxygen peaks were very small compared to the other measured peaks and were thus considered as trace components in the final analysis.

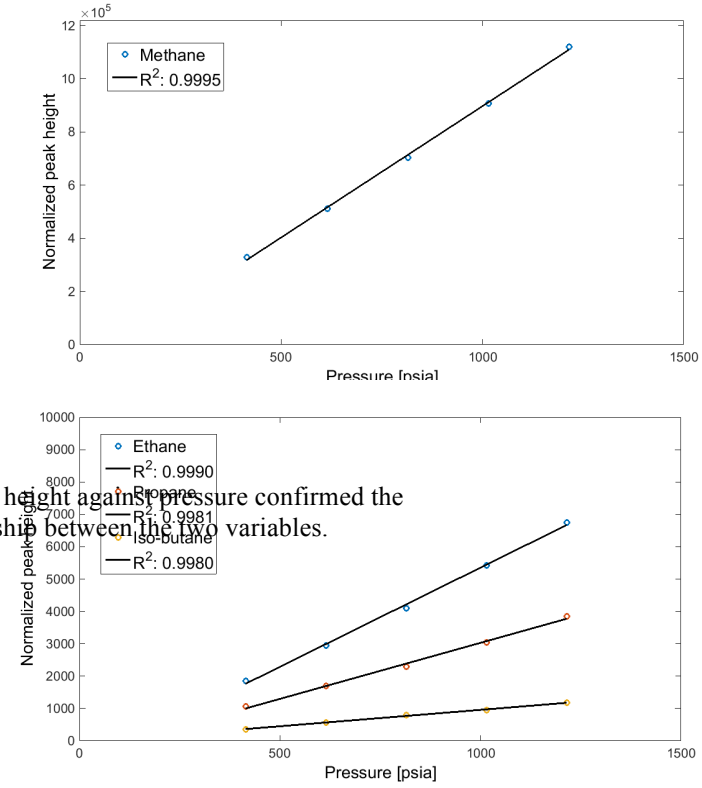

Figure 5: Plotting peak height against pressure confirmed the suspected linear relationship between the two variables.

The fact that Raman intensities do not directly correspond to concentration but are also factors of laser power and molecular scattering cross-sections necessitated the use of ratios to calculate relative concentrations (Subramanian 2000, White 2006, Coward 2011). Because peak height increased linearly with pressure for every sample component, the ratio of one peak height to another in a given sample with set molar ratios remained constant. This simple relationship allowed for the use of peak height ratios to determine molar ratios. A series of standard gas mixtures was used that were either characterized by gas

chromatography or prepared by weight. These enabled creation of calibration curves and ratios that related peak height ratios to molar ratios (Figure 6). Each gas was referenced to methane, the dominant component of the samples. As many standards as possible were used to create the calibration curves and solve for the simple ratio between peak height ratio and molar ratio, known as the molar response factor (MRF) (Table 2). The number of available standards containing both methane and another sample component gas ranged from only one for carbon dioxide and nitrogen, to two for propane and iso-butane, to four for ethane.

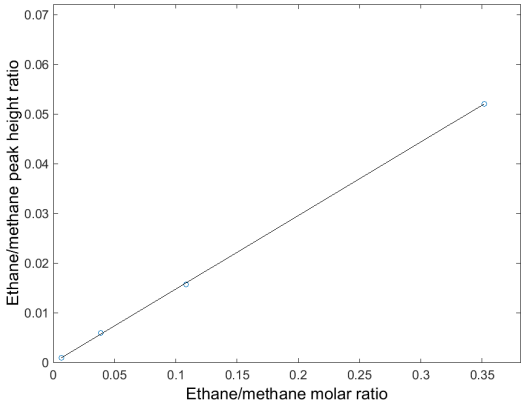

Figure 6 – Four standards that contained methane and ethane allowed for the creation of a calibration curve that plotted ethane to methane peak height ratio against ethane to methane molar ratio. The resulting regression line had an R^2 value of 0.99995.

Table 2 – The molar response factor for each of the gas components relative to methane.

Peak height ratio	**MRF**
ethane/methane	0.14798
propane/methane	0.17899
iso-butane/methane	0.19323
carbon dioxide/methane	0.28491
nitrogen/methane	0.18760

A linear regression on the ethane to methane calibration curve resulted in an uncertainty of less than 1% in the MRF. An uncertainty of over 100% in the y-intercept made the intercept statistically insignificant. Using the equations of the

line for ethane, propane, and iso-butane and using a simple ratio between MRF and peak height ratio for carbon dioxide and nitrogen allowed for subsequently determining the molar percentages of each sample using equations (1) through (5). The intercept could not be shown to be statistically insignificant for equations formed from connecting only two calibration points, though they were very close to 0.

$$Peak\ height\ ratio = MRF \bullet molar\ ratio + intercept \quad (1)$$

$$Molar\ ratio = \frac{Peak\ height\ ratio - intercept}{MRF} \quad (2)$$

$$Total\ mols = mols_A + mols_B + mols_C + \cdots \quad (3)$$

$$\frac{Total\ mols}{mols_A} = 1 + \frac{mols_B}{mols_A} + \frac{mols_C}{mols_A} + \cdots \quad (4)$$

$$\frac{mols_A}{Total\ mols} \times 100\% = \%\ A = \left(\frac{Total\ mols}{mols_A}\right)^{-1} \quad (5)$$

2. SAMPLE COMPOSITIONS

Calculation of MRFs allowed for computation of mole percentages that accounted for all detectable components of the gas samples. In addition to free gases from vents, samples of decomposed hydrates and in-situ spectra of free gas, gas evolved from oil, and hydrates composed the complete dataset (Tables 3-8). A version of the MATLAB code modified to subtract background seawater spectra was used to analyze in-situ spectra with seawater peaks.

Table 3 – Three gas samples from North Slump vents were collected with the ROV *Doc Ricketts* (DR). DR531 spectra were acquired in-situ.

North Slump free gas	% CH_4	% C_2H_6	% C_3H_8	% C_4H_{10}	% CO_2	% N_2	% O_2
DR653 blue	97.91	0	0	0	1.06	1.03	trace
DR531 000008	93.58	0	0	0	0.92	5.50	trace
DR531 000012	95.65	0	0	0	1.44	2.91	trace

Table 4 – Five gas samples were collected from South Slump vents.

South Slump free gas	% CH_4	% C_2H_6	% C_3H_8	% C_4H_{10} (iso)	% CO_2	% N_2	% O_2
DR652 red	90.44	2.93	1.29	0.29	2.76	2.29	trace
DR652 blue	89.67	2.98	1.66	0.37	3.27	2.05	trace
DR652 black	92.04	3.09	2.18	0.55	0.94	1.20	trace
DR514 G-11	92.93	0.64	0.76	0.14	4.05	1.48	trace
DR514 G-12	92.98	0.60	0.68	0.16	4.10	1.48	trace

Table 5 – Two hydrate samples from the North Slump were decomposed and collected with the heated funnel for laboratory analysis.

North Slump decomposed hydrate	% CH_4	% C_2H_6	% C_3H_8	% C_4H_{10} (iso)	% CO_2	% N_2	% O_2
DR653 red	98.14	0	0	0	0.68	1.18	trace
DR653 black	98.21	0	0	0	0.68	1.11	trace

Table 6 – Both in-situ and laboratory spectra were acquired of decomposed hydrate from the North Slump.

DR653 black	% CH_4	% C_2H_6	% C_3H_8	% C_4H_{10} (iso)	% CO_2	% N_2	% O_2
In-situ	98.46	0	0	0	0.59	0.94	0
Laboratory	98.21	0	0	0	0.68	1.11	trace

Table 7 – In-situ spectra of North Slump hydrate were acquired on two expeditions.

North Slump hydrate	% CH_4	% C_2H_6	% C_3H_8	% C_4H_{10} (iso)	% CO_2	% N_2	% O_2
DR531 000006	95.31	0	0	0	1.87	2.82	0
DR654 000012	97.30	0	0	0	0.49	2.21	trace

Table 8 – In-situ spectra of the gas evolving from South Slump oil were acquired as *Doc Ricketts* ascended.

South Slump gas from oil	% CH_4	% C_2H_6	% C_3H_8	% C_4H_{10} (iso)	% CO_2	% N_2	% O_2
At 600 m	85.44	2.23	0.52	0.12	2.68	9.01	trace
At 500 m	84.99	2.37	0.65	0.06	2.80	9.13	trace
At 200 m	86.34	2.74	0.63	0.25	2.60	7.44	trace

DISCUSSION

1. ANALYSIS OF METHOD DEVELOPMENT

A low volume pressure boosting system made of stainless steel tubing and needle valves enabled laser Raman analysis of gases sampled from the seafloor. The Swagelok fittings and O-rings made for a tight system that held a vacuum for multiple hours. The system was tested up to 1200.0 psig and only fluctuated in, at most, 0.4 psig during the course of an experiment. Such small pressure variation did not necessarily indicate a leak, but could have also resulted from slight temperature changes in the system outside of the temperature-controlled pressure cell. The booster cylinder was capable of increasing the initial pressure of the sample gas by more than six-fold: typically a sample was boosted from about 200 psig to the highest target pressure of 1200.0 psig. If a low initial pressure necessitated additional pressure boosting, the system of valves allowed for isolation of pressurized sample gas in the pressure cell while the booster was opened to the sample cylinder for a second loading. These subsequent passes with the booster were not capable of dramatically increasing the sample pressure, but did allow for the measurement of samples with initial pressures below 200 psig. Pressure boosting amplified small peaks in the spectra so that peaks heights three orders of magnitude smaller than the tallest peak were visible.

Analyzing the sample compositions relied on the linear relationship that was observed between peak height and pressure, at least in the range of pressures investigated. This relationship signified the pressure independence of peak height ratios. This realization was crucial because the partial pressures of various gases

varied significantly across the standards and samples. For in-situ Raman experiments during which scientists lack precise control over conditions, this pressure-independent relationship is very useful. Peak area was also considered as a possible metric, but peak height values proved to be more linear and easier to calculate above baseline noise.

The calibration curve for the ethane to methane molar ratio demonstrated that peak height ratios served as a precise proxy for molar ratio with an uncertainty of only 0.7251%. This small margin of uncertainty suggests that scientists can successfully and fairly easily use LRS to make quantitative measurements of gases, despite the widespread use of LRS as a qualitative technique. The use of standards similar in concentration to samples in order to create a calibration curve enables this quantitative analysis. Because only two standards were available to solve for propane to methane and iso-butane to methane, it was not possible to determine the statistical significance of the y-intercept or calculate the uncertainty in the MRF. For the carbon dioxide and nitrogen ratios, for which only one standard was available, it was impossible to perform a linear regression and the y-intercept was assumed to be 0. In reality, there is likely greater uncertainty in the molar ratios of propane, iso-butane, carbon dioxide, and nitrogen to methane in comparison with the ethane to methane ratio.

2. ANALYSIS OF SAMPLE COMPOSITIONS

The compositions of the samples of vent gas and decomposed hydrate from Eel River Canyon showed some interesting temporal and spatial patterns. Gases from the South Slump in 2014 contain roughly 3% ethane, 1-2% propane, and 0.3-0.6% iso-butane (Table 4, DR652 samples). Gases from the South Slump in 2013 contain these components in smaller quantities: roughly 0.6% ethane, 0.7% propane, and 0.15% iso-butane (Table 4, DR514 samples). The apparent increase in the concentration of multiple-carbon alkanes at the South Slump from 2013 to 2014 may indicate that the composition of the venting gases changes slightly over time.

Gases from the North Slump in 2014 (DR653 sample) and 2013 (DR531 samples) contained no detectable multiple-carbon alkanes (Table 3). Though it is possible that the hydrocarbon gas mixture is complex at the North Slump, levels of alkanes other than methane are either below the lower limit of detection of the LRS system or are, in fact, absent altogether. This absence of detectable multiple-carbon alkanes is consistent with their absence in decomposed hydrate samples from the North Slump in 2014 (Table 5). The small dataset prohibits strong conclusions about temporal and spatial patterns in the gas compositions at Eel River Canyon, but preliminary data does indicate that significant differences may exist.

The MATLAB routine allowed for quantitative processing of in-situ spectra of various Eel River Canyon materials to compliment the spectra acquired in the laboratory. An in-situ spectrum of one of the decomposed hydrate sample gases provided a comparison between LRS analysis in-situ versus in the laboratory (Table 6). While the in-situ spectrum indicated that the gas contained no detectable oxygen, the laboratory spectrum showed that the gas contained a trace amount of oxygen, as well as greater amounts of nitrogen and carbon dioxide. This comparison suggests that a slight contamination of the decomposed hydrate occurred either through contact with seawater or with residual air in the sample cylinders. This example shows that in-situ spectra provide the most accurate picture of gases from the seafloor.

In-situ spectra of hydrate from the North Slump acquired during two ROV dives added another dimension to the dataset. In order to process these spectra, an additional script was written to subtract a seawater background spectrum from the hydrate spectra that contained overlapping water and CH stretches. Because the peak shapes of water in hydrate form bear differences to the peak shapes of water in liquid form, the subtraction method did not produce a perfectly resolved difference spectrum. The in-situ spectra appear very similar to those of decomposed hydrates. An apparent oxygen peak in the in-situ spectrum DR654 000012 might actually be the υ_2 stretching peak from methane that partially overlaps with the oxygen peak. A comparison of the free gas spectra to the

hydrate spectra must consider that the calculated MRFs only strictly apply to the components in gaseous form and may be slightly different from the gases in the hydrates.

Finally, the free gas was compared to the gas dissolved in an oil sample from the South Slump using spectra acquired at three depths as the gas evolved from the oil during ROV ascent (Figure 7) (Table 8). This gas appears less enriched in methane and more enriched in nitrogen than the vent gas or hydrates. The greater proportion of multiple-carbon alkanes to methane in the gas from the oil compared to the vent gas is consistent with the fact that oil is composed of higher-carbon alkanes. A direct comparison of the spectrum taken at 600 m below the surface to that taken at 200 m below the surface shows that the gas becomes slightly enriched in ethane, propane, and iso-butane under less pressure at a shallower depth. This is consistent with the higher alkanes being preferentially soluble in the liquid phase at higher pressures and only being released into the gas phase at low pressures due to their low vapor pressures.

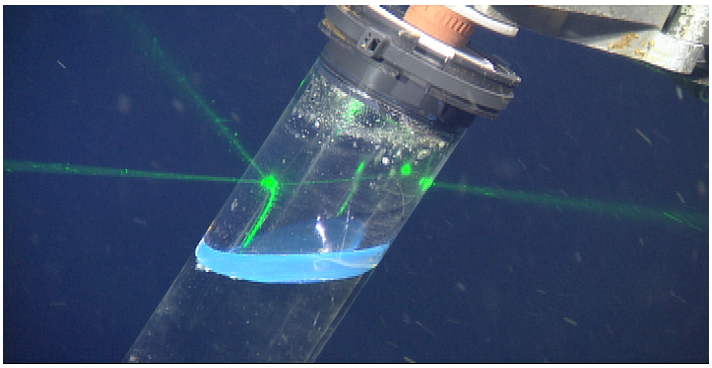

Figure 7 – The laser focused on the gas headspace above the oil that increased in volume as the ROV ascended to lower pressure conditions.

CONCLUSIONS/RECOMMENDATIONS

In conjunction with a pressure boosting system, LRS is a useful technique for studying deep sea gases in the laboratory. The pressure booster enables detection of traces gases and quantitation of peaks above baseline noise. Using peak height ratio as a proxy for molar ratio allows for quantitative measurements using LRS, given the availability of well-characterized standards to make a

calibration curve. An analysis of samples from Eel River Canyon indicated that the composition of gases emanating from the seafloor vents may change over time. Gas mixtures appear more complex at the South Slump site, as was expected from the discovery of sII hydrate in that location. Gas dissolved in oil from the South Slump appears to have higher concentrations of multiple-carbon alkanes and nitrogen relative to methane. Laboratory spectra of decomposed hydrates and in-situ spectra of hydrates from the North Slump were consistent with the laboratory spectra of vent gas, none of which contain detectable amounts of multiple-carbon alkanes. Comparison of an in-situ spectrum with a laboratory spectrum of the same sample revealed that, while in-situ measurements may be more technically challenging, they provide more certain results due to the decreased chances of sample contamination.

This project showed that scientists can successfully use LRS in the laboratory for quantitative analysis of pressurized gases. In order to improve the methods described in this paper, a booster with a higher pressure rating could enable detection of more trace gases as well as improve the quantitation of small peaks. Using MRFs specifically for gases in hydrates, though difficult to determine, would correct the reported values for hydrate composition. Obtaining more standards would improve the calibration curves and determine the uncertainty in the molar ratios. Future in-situ LRS measurements of deep sea gases could use the MATLAB routine developed in this project and the laboratory measured MRFs to determine gas composition in real time under any pressure conditions. The continued study of the geochemistry of Eel River Canyon and similar locations will enhance knowledge of the dynamics of materials from the seafloor in both the ocean and the atmosphere.

ACKNOWLEDGEMENTS

This project was completed under the generous mentorships of Peter Brewer, Edward Peltzer, and Peter Walz. Thanks are given to the crew of the R/V *Western Flyer* and ROV *Doc Ricketts*, as well as to the scientific teams of Peter

Brewer and Charlie Paull, for collecting and supplying the gas samples. George Matsumoto and Linda Kuhnz directed the internship program under which this research was completed at the Monterey Bay Aquarium Research Institute, with funding from the David and Lucile Packard Foundation.

References:

Brewer, P.G., Malby, G., Pasteris, J.D., White, S.N., Peltzer, E.T., Wopenka, B., Freeman, J., and Brown, M.O. (2004). Development of a laser Raman spectrometer for deep-ocean science. *Deep-Sea Research I*, **51**: 739-753.

Coward, E. (2011). Rates of CH_4 Displacement by a N_2-CO_2 Mixture in CH_4 Hydrates. MBARI Intern Papers.

Gardner, J.V., Malik, M., and Walker, S. (2009). Plume 1400 Meters High Discovered at the Seafloor off the Northern California Margin. *Eos*, **90**: 275.

Gwiadza, R., Paull, C.K., Caress, D.W., Lundsten, E., Anderson, K., and Thomas, H. (2011). Seafloor Morphology Associated with Deep-Water Gas Plumes Near Eel Canyon. American Geophysical Union, Fall Meeting 2011, abstract #OS13B-1529.

Hovland, M., Jensen, S., and Fichler, C. (2012). Methane and minor oil macro-seep systems – Their complexity and environmental significance. *Marine Geology*, **332-334**: 163-173.

Monterey Bay Aquarium Research Institute 2013 Annual Report.

Rehder, G., Leifer, I., Brewer, P.G., Friederich, G., and Peltzer, E.T. (2009). Controls on methane bubble dissolution inside and outside the hydrate stability field from open ocean field experiments and numerical modeling. *Marine Chemistry*, **114**: 19-30.

Shimanouchi, T. (1972). Tables of Molecular Vibrational Frequencies Consolidated Volume I. National Standard Reference Data System, National Bureau of Standards, NSRDS-NBS 39.

Subramanian, S. (2000). Measurements of Clathrate Hydrates Containing Methane and Ethane Using Raman Spectroscopy. PhD thesis, Colorado School of Mines, Golden.

Walz, P.M., Peltzer, E.T., Gwiazda, R., Anderson, K., Paull, C.K., Brewer, P.G., Lorenson, T.D., Grim, R.G., and Sum, A.K. (2014). In Situ and Laboratory Raman Observations of an Oil Associated Gas Hydrate in the Eel River Basin. *Proceedings of the 8th International Conference on Gas Hydrates*.

White, S.N., Brewer, P.G., Peltzer, E.T. (2006). Determination of gas bubble fractionation rates in the deep ocean by laser Raman spectroscopy. Marine Chemistry, **99**: 12-23.

Zhang, X., Kirkwood, W.J., Walz, P.M., Peltzer, E.T., and Brewer, P.G. (2012). A Review of Advances in Deep-Ocean Raman Spectroscopy. *Applied Spectroscopy*, **66**: 237-249.